JOURNAL OF Materials CHEMISTRY

Preparation of pyrite thin films by atmospheric pressure chemical vapor deposition using $FeCl_3$ and CH_3CSNH_2

Naoyuki Takahashi,* Takehiko Sawada, Takayuki Nakamura and Takato Nakamura

Department of Materials Science and Technology, Faculty of Engineering, Shizuoka University, 3-5-1 Johoku, Hamamatsu 432-8561, Japan.
E-mail: takanao@mat.eng.shizuoka.ac.jp; Fax: +81-53-478-1197

Received 14th April 2000, Accepted 19th July 2000
First published as an Advanced Article on the web 7th September 2000

A new vapor-phase deposition method using $FeCl_3$ and CH_3CSNH_2 as starting materials has been examined for the growth of FeS_2 films on glass substrates under atmospheric pressure. The X-ray diffractogram of the as-deposited films at 773 K showed a typical cubic pyrite pattern. The growth rate was approximately 8.4 μm h^{-1} at 773 K. The resulting films have a carrier concentration of 6.5×10^{18} cm^{-3} and a Hall mobility of 20 cm^2 V^{-1} s^{-1} at 298 K.

1 Introduction

Pyrite (FeS_2) has received growing attention in the last decade as one of the promising materials for solar energy applications[1,2] such as depolarizer anodes for hydrogen production[3] and cathodes in high-energy-density batteries.[4,5] Therefore the physical[6] and chemical[7] properties of natural and synthetic crystals have been widely studied so far.

Thin films of FeS_2 have been prepared by means of chemical vapor deposition (CVD),[8–10] magnetron sputtering[11] and thermal sulfidation of metallic iron[12,13] as shown in Table 1. However, these methods are costly because of the films being deposited *in vacuo* using expensive set-ups and chemicals. In addition, the growth rate is too slow to be applied to industrial production.

For this reason, the purpose of this study is to develop an alternative method using $FeCl_3$ and CH_3CSNH_2 as starting materials for the growth of FeS_2 films. This brings the following advantages: (a) the films are formed by a simple reaction of $FeCl_3$ with CH_3CSNH_2 in the gas phase under atmospheric pressure; (b) their post-annealing is not necessary; (c) high-purity $FeCl_3$ used as an iron source is cheap compared with the source materials for the deposition techniques described above.

2 Experimental

A schematic illustration of the reactor used in this study is shown Fig. 1. $FeCl_3$ and CH_3CSNH_2 were evaporated from the source boats at temperatures of 503 and 393 K, respectively, and were carried to the growth zone (purified N_2 was used as the carrier gas). Thin films of FeS_2 were deposited onto the glass surface in the hot-wall horizontal quartz reactor by the reaction of $FeCl_3$ with CH_3CSNH_2 under atmospheric pressure. Typical growth conditions are summarized in Table 2. The flow rate of the N_2 carrier gas is given in Fig. 1. X-Ray diffraction (XRD) analysis using a Rigaku Denki diffractometer with Cu Kα radiation was carried out in order to identify the crystal structure of the resulting films. Reflection Fourier transform infrared spectroscopy (FT-IR) using a Shimadzu FTIR-8000 instrument was applied to assay trace amounts of impurities in the films and to perform phase identification as well. Infrared spectra were measured in the range of 200 to 5000 cm^{-1}. Scanning electron micrographs (SEM) were recorded on a Shimadzu Superscan instrument in order to estimate the film thickness and to observe the surface morphology. The chemical composition of the film was determined by energy-dispersive analysis of X-rays (EDAX) using a JEOL Ltd. JXA-8900R instrument, in which the data were calibrated with a FeS_2 single crystal of known stoichiometry. The electrical resistivity (ρ) was measured by means of a four-probe technique. Tungsten wire springs (0.5 mm diameter) with platinum solder at the ends were used to provide ohmic contact between the film and the probes. Hall coefficients (R_H) were measured at a magnetic field of 0.7 T.

3 Results and discussion

Fig. 2 shows a typical X-ray diffraction profile of the film deposited at 773 K together with those of pyrite, marcasite and $Fe_{1-x}S$ as cited in the JCPDS files. It is obvious that the observed diffraction lines can be assigned to pyrite with a cubic structure. There is no indication of either marcasite or $Fe_{1-x}S$ being present in the film. The lattice constant, calculated to be $a = 0.5405$ nm, is slightly larger than the reported value of 0.5417 nm.[14] A similarly large lattice constant was also estimated from the XRD pattern of the film at 723 K.

At 798 and 823 K, in contrast, $Fe_{1-x}S$ was formed, implying that FeS_2 with the cubic structure transforms to $Fe_{1-x}S$ due to

Table 1 Vapor-phase deposition methods of FeS_2 films reported

Growth method	Fe source	S source	Growth rate/μm h^{-1}	Pressure/atm
Low-pressure CVD[a]	$Fe(CO)_5$	TBS[f], TBDS[g]	10	10^{-3}
MOCVD[b]	$Fe(CO)_5$	TBDS[g]	0.7	4.9×10^{-2}
MOCVD[c]	$Fe(CO)_5$	H_2S	2	4.9×10^{-2}
Magnetron sputtering[d]	FeS_2 target		0.26	10^{-5}
Thermal sulfidation of iron film[e]	Fe film	S	—	10^{-9}

[a]Ref. 8. [b]Ref. 9. [c]Ref. 10. [d]Ref. 11. [e]Refs. 12 and 13. [f]TBS: *tert*-butyl sulfide. [g]TBDS: *tert*-butyl disulfide.

 DOI: 10.1039/b003015p

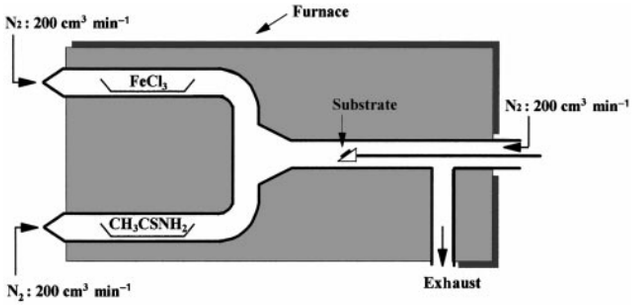

Fig. 1 Schematic diagram of the apparatus used in this work.

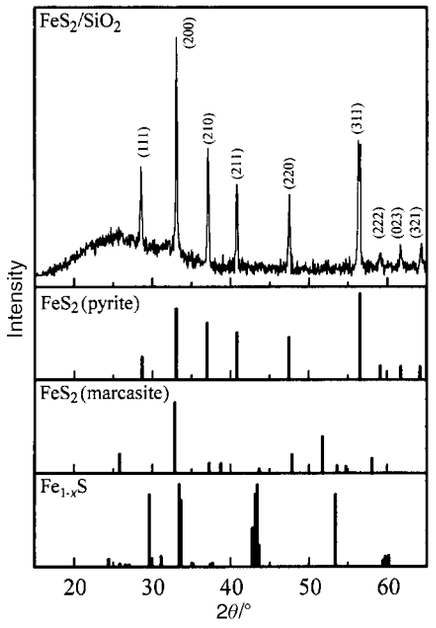

Fig. 2 X-Ray diffraction pattern of the film deposited at 773 K and those of pyrite (JCPDS 6-710), marcasite (JCPDS 3-799) and $Fe_{1-x}S$ (JCPDS 29-723) powders.

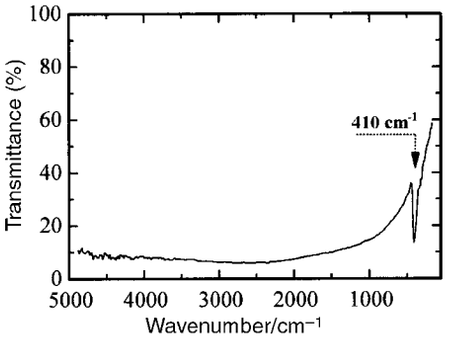

Fig. 3 FT-IR spectrum of the as-deposited pyrite film at 773 K.

the evolution of S above 773 K. Schleich and Chang[8] and Thomas *et al.*[9] have reported similar transformations during the preparation of pyrite film by low pressure CVD (LP-CVD) and metal organic CVD (MOCVD), respectively.

Fig. 3 shows an FT-IR spectrum of the as-deposited pyrite film at 773 K. A signal corresponding to the stretching mode of the S–S bond due to pyrite appeared at 410 cm^{-1}, and no other absorption was observed.[8]

Table 2 Typical growth conditions

Substrate	Glass
$FeCl_3$ source temperature	503 K
CH_3CSNH_2 source temperature	383 K
Carrier gas	N_2
Total flow rate	600 cm^3 min^{-1}
Growth temperature	723–823 K

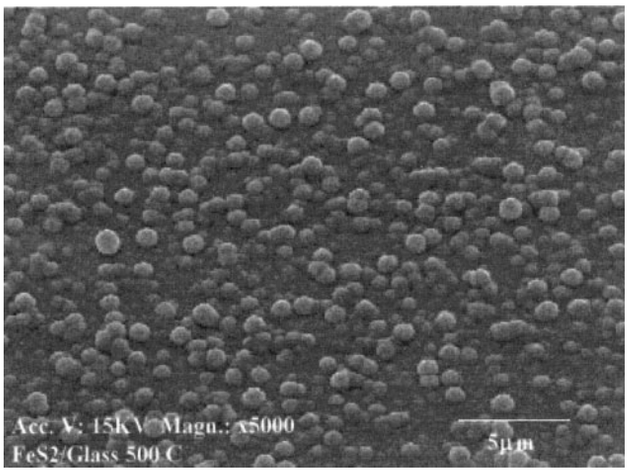

Fig. 4 A SEM image of the pyrite film surface deposited at 773 K.

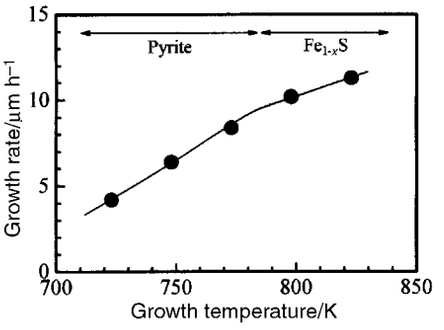

Fig. 5 Plots of the growth rate of films as a function of growth temperature.

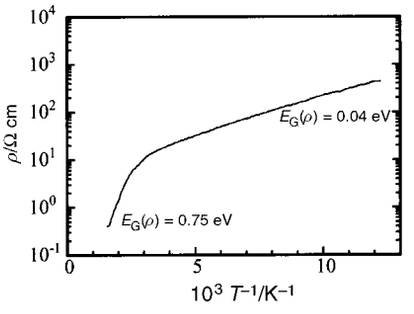

Fig. 6 Temperature dependence of the electrical resistivity of the as-grown pyrite film at 773 K.

In Fig. 5, the growth rate of the pyrite film is plotted as a function of the growth temperature. As the temperature is increased from 723 to 823 K, the rate increases monotonically from 4.2 to 11.4 μm h^{-1}. At 798 K, the slope of the curve decreases, implying that pyrite transforms to $Fe_{1-x}S$ with the

evolution of S. For the pyrite film the maximum growth rate was approximately 8.4 μm h^{-1} at 773 K. This is higher than those prepared by MOCVD[9,10] and magnetron sputtering,[11] but it is comparable to that deposited by low pressure CVD.[8] Therefore, the present $FeCl_3$–CH_3CSNH_2 system is of promise for the preparation of pyrite films with high growth rates.

Fig. 6 shows the temperature dependence of the electrical resistivity (ρ) of the as-deposited pyrite film at 773 K. As is seen in Fig. 6, the film is semiconductive over the wide temperature range of 77 to 600 K. This feature is almost the same as that of the single crystal reported by Bither *et al.*[14] Also, the electrical resistivity is reported to be 10 Ω cm at 298 K.

The energy gap $E_G(\rho)$ is expressed as the equation $\rho = \rho_0 \exp(E_G/2\kappa_B T)$, in which κ_B is Boltzmann's constant. $E_G(\rho)$ is estimated to be 0.75 and 0.04 eV in the high and low temperature regions, respectively, by utilizing the variation of $\log \rho$ with $1/T$ in Fig. 6. The $E_G(\rho)$ value of 0.75 eV obtained in the high temperature region is comparable to the values reported by Horita[15,16] and Marinace,[17] which corresponds to the energy gap between the valence band and conduction band. In the low temperature region, on the other hand, $E_G(\rho)$ was estimated to be 0.04 eV, being ascribed to the impurity levels.

The carrier concentration and Hall mobility of the as-deposited film were 6.5×10^{18} cm^{-3} and 20 cm^2 V^{-1} s^{-1} at 298 K, respectively. The obtained carrier concentration is similar to those of pyrite films prepared by other methods.[10,11] In contrast, the Hall mobility is small compared with the reported electron mobility of 300 cm^2 V^{-1} s^{-1}.[18] This discrepancy may be attributed to the crystalline quality of the pyrite film.

4 Conclusion

Thin films of pyrite were deposited on a glass substrate under atmospheric pressure by a new vapor-phase deposition method using $FeCl_3$ and CH_3CSNH_2 as source materials. As-deposited films prepared in the temperature range from 723 to 773 K showed a typical X-ray diffraction pattern of pyrite with a cubic structure. The maximum growth rate was approximately 8.4 μm h^{-1} at 773 K. Their electrical conductivity, carrier concentration and Hall mobility at 298 K were 10 Ω cm, 6.5×10^{18} cm^{-3} and 20 cm^2 V^{-1} s^{-1}, respectively. Consequently, it is evident that reaction of $FeCl_3$ and CH_3CSNH_2 under atmospheric pressure yields high-quality pyrite films with rapid growth rates.

References

1 W. Jaegermann and H. Tributsch, *J. Appl. Electrochem.*, 1983, **13**, 743.
2 A. Ennaoui and H. Tributsch, *Solar Cells*, 1984, **13**, 197.
3 S. B. Lalvani and M. Shami, *J. Electrochem. Soc.*, 1986, **133**, 1364.
4 C. A. Vincent, *Modern Batteries*, Edward Arnold, London, 1984, p. 182.
5 S. S. Wang and R. N. Seefurth, *J. Electrochem. Soc.*, 1987, **134**, 530.
6 A. L. Echarri and C. Sanchez, *Solid State Commun.*, 1974, **15**, 827.
7 A. N. Buckler and R. Woods, *Appl. Surf. Sci.*, 1987, **27**, 437.
8 D. M. Schleich and H. S. W. Chang, *J. Cryst. Growth*, 1991, **112**, 737.
9 B. Thomas, C. Hopfner, K. Ellmer, S. Fiechter and H. Tributsch, *J. Cryst. Growth*, 1995, **146**, 630.
10 B. Thomas, K. Ellmer, M. Muller, C. Hopfner, S. Fiechter and H. Tributsch, *J. Cryst. Growth*, 1997, **170**, 808.
11 G. Willeke, R. Dasbach, B. Sailer and E. Bucher, *Thin Solid Films*, 1992, **213**, 271.
12 S. Bausch, B. Sailer, H. Keppner, G. Willeke, E. Bucher and G. Frommeyer, *Appl. Phys. Lett.*, 1990, **57**, 25.
13 I. J. Ferrer and C. Sanchez, *J. Appl. Phys.*, 1991, **70**, 2641.
14 T. A. Bither, R. J. Bouchard, W. H. Cloud, P. C. Donohue and W. J. Siemens, *Inorg. Chem.*, 1968, **7**, 2208.
15 H. Horita, *Jap. J. Appl. Phys.*, 1971, **10**, 1478.
16 H. Horita, *J. Phys. Soc. Jpn.*, 1972, **33**, 1723.
17 J. C. Marinace, *Phys. Rev.*, 1954, **96**, 593.
18 A. M. Karguppikar and A. G. Vedeshwar, *Phys. Status Solidi A*, 1988, **109**, 549.